

Article

Nanoreinforced Cast Al-Si Alloys with Al₂O₃, TiO₂ and ZrO₂ Nanoparticles

Iman S. El-Mahallawi ^{1,*}, Ahmed Yehia Shash ^{2,*} and Amer Eid Amer ³

¹ Mining Petroleum and Metallurgical Engineering Department, Cairo University, Giza 12613, Egypt

² Mechanical Design and Production Department, Cairo University, Giza 12613, Egypt

³ Mechanical Design and Production Engineering Department, Faculty of Engineering, Beni-Suef University, Beni-Suef 62111, Egypt; E-Mail: aeid958@yahoo.com

* Authors to whom correspondence should be addressed;

E-Mails: ielmahallawi@bue.edu.eg (I.S.E.-M.); ahmed.shash@cu.edu.eg (A.Y.S.);

Tel.: +20-10-0604-4661 (I.S.E.-M.); +20-23567-8516 (A.Y.S.).

Academic Editor: Anders E. W. Jarfors

Received: 20 April 2015 / Accepted: 11 May 2015 / Published: 20 May 2015

Abstract: This study presents a new concept of refining and enhancing the properties of cast aluminum alloys by adding nanoparticles. In this work, the effect of adding alumina (Al₂O₃), titanium dioxide (TiO₂) and zirconia (ZrO₂) nano-particles (40 nm) to the aluminum cast alloy A356 as a base metal matrix was investigated. Alumina, titanium dioxide and zirconia nano-powders were stirred in the A356 matrix with different fraction ratios ranging from (0%–5%) by weight at variable stirring speeds ranging from (270, 800, 1500, 2150 rpm) in both the semisolid (600 °C) and liquid (700 °C) state using a constant stirring time of one minute. The cast microstructure exhibited change of grains from dendritic to spherical shape with increasing stirring speed. The fracture surface showed the presence of nanoparticles at the interdendritic spacing of the fracture surface and was confirmed with EDX analysis of these particles. The results of the study showed that the mechanical properties (strength, elongation and hardness) for the nanoreinforced castings using Al₂O₃, TiO₂ and ZrO₂ were enhanced for the castings made in the semi-solid state (600 °C) with 2 weight% Al₂O₃ and 3 weight% TiO₂ or ZrO₂ at 1500 rpm stirring speed.

Keywords: nanoreinforced castings; semisolid casting; hypoeutectic aluminum alloys

1. Introduction

Al-Si alloys are used for several automotive applications and various aerospace industries due to their outstanding properties such as high castability, abrasion resistance and excellent strength to weight ratio. The Al-Si alloys in particular are greatly known for their rapidly advancing activities in aircrafts, aerospace and automotive industries. Intensive efforts have been made to understand the modification of these alloys by adding Na, Sr or Sb [1–4]. The addition of certain elements, such as calcium, sodium, strontium, and antimony, to hypoeutectic aluminum-silicon alloys results in a finer lamellar or fibrous eutectic network [4]. Gruzleski *et al.* [2] discussed the techniques commonly used in the foundry, and showed that the addition of P to the melt results in modified hypereutectic Al-Si alloys, with both coarse and unmodified eutectic silicon surrounding the refined primary silicon. Though Na and Sr are used to achieve refinement of the eutectic silicon, a combined effect does not happen at the same time with P due to chemical incompatibility of phosphorus with other modifying chemicals such as strontium and sodium. This has been explained [2] to result from the formation of strontium phosphide or sodium phosphide upon the addition of strontium or sodium to phosphorus pre-refined alloys. Other investigations have shown that adding rare earth elements would result in modification and refinement of the primary and eutectic silicon particles [5,6].

The mechanical properties of the A356 alloy, not only depend on the dendritic structures, but also on the sizes and morphologies of the eutectic Si particles [7,8]. The eutectic Si of untreated A356 presents a coarse plate-like structure, which will deteriorate the mechanical properties (especially the ductility) of the alloy. The mechanical properties of the hypereutectic Al-Si alloys are highly affected by the morphology, size, and distribution of both primary Si particles (PSPs) and eutectic silicon. The morphology of silicon particles is dependent on the solidification rate, as under normal casting conditions, PSPs are very coarse and show star-like and other irregular shapes. Therefore, to improve the mechanical properties of the hypo and hypereutectic Al-Si alloys, size, distribution, and the morphology of PSPs and eutectic silicon should be controlled, as well as refining of the aluminum dendrites [2,3].

The use of ceramic particles to improve the yield and ultimate strength (UTS) of cast Al alloys has been considered by many researchers [9–15]. Prospects of using nanoparticles as refining and reinforcement agents to gain improved performance of Al-Si cast alloys by adding Al_2O_3 and TiO_2 particles have gained significant interest recently [16–22].

Rohatgi *et al.* [11] have predicted the significant role of producing Al-Si ceramic composites for bearings, pistons, cylinder liners, *etc.* leading to savings in materials and energy. Previous trials to modify the structure and enhance the mechanical properties of A356 via reinforcement with ceramic micro-sized particles, such as Al_2O_3 [12], SiC [13,14] and TiC [15] did not result in a breakthrough in casting modification, though a few engineering cast products entered the market [23].

It has been shown that enhanced as-cast properties of Al-Si alloys are obtained by treating the melt with nano-sized particles [16–22]. Introducing Al_2O_3 nanoparticles to the (A356) cast alloy in the semi-solid state with mechanical stirring has a beneficial effect on improving the strength–ductility relationship in these alloys [16,17]. This is attributed to the modification of the dendritic columnar structure into a smaller and equiaxed globular grain arrangement, resulting from semi-solid casting conditions. Moreover, the enhanced viscosity of the semi-solid processing would serve to improve the ceramic particle/melt wettability and entrap or capture the reinforcement material physically. The addition of

ceramic particles to aluminum alloys raises the viscosity very quickly [24], providing suitable conditions for particle capture; moreover, the Al_2O_3 nanoparticles possess appropriate properties that are compatible with the Al alloy relatively high thermal conductivity and thermal expansion coefficients that affects its role as a nanodispersion for reinforcement in the Al alloy matrix [16–19].

For most applications, a homogeneous distribution of the particles is desirable in order to maximize the mechanical properties. In order to achieve a good homogeneous distribution of the particles in the matrix, the process parameters related with the stir casting method must be considered, the stirring speed and stirring time are key parameters. There is some debate in literature about the appropriate stirring speeds, while one study [25] has investigated stirring speeds within the range of 500, 600 and 700 rpm and the stirring times in the range of 5, 10 and 15 min, another study [26] has used higher stirring speeds in the range 1000–1500 rpm.

Haizhi Ye [23] has presented an overview of Al-Si based alloys for engine applications where it was shown that fatigue failure and wear caused by surface delamination are the most important causes for failure or end of life of engine parts. The main causes according to the analysis presented by Haizhi Ye [23] are the size and shapes (morphology) of the Primary Si Particles (PSPs). Also, these materials have low specific gravity that makes their properties particularly superior in strength and modulus to many traditional engineering materials.

Therefore, the aim of this work is to compare the effect of adding three different nanoparticles as reinforcements (Al_2O_3 , TiO_2 and ZrO_2) on the microstructure, the mechanical properties and the wear behavior of A356 aluminum alloy cast from the semi-solid state. The ultimate goal of the work is to discuss the options for producing nanocomposites via the casting route, in order to evaluate the options for using nanoparticles dispersion for the production of semi-solid cast A356 alloy with improved properties.

2. Statistical Analysis

The first step in this work was to statistically-analyze the results obtained through previous work by the authors (represented by nine samples for each condition), for A356 alumina (Al_2O_3) nanoreinforced cast alloys [16–18], on the relation between the tensile strength and the amount of nanoparticles added (in weight%) and the addition temperature. The ANOVA technique was applied on the responses to find fisher factors (f) and compare it with the tabulated values at the levels of confidence (90%, 95%, and 99%), using response surface methodology (RSM) technique. Table 1 shows the orthogonal array L4 that was used to apply the ANOVA technique. The obtained results showed that the effect of nano-reinforcement is significant at 90%, and the effect of the temperature is significant at 85%. The analysis results were used to predict the measured values. Accordingly, the following experimental plan was made for this work.

Table 1. Orthogonal L4 array for ANOVA analysis of previous results.

Trial number	Factor	Nano%	Stirring Temperature	Predicted Tensile Strength	Average Value of Measured Tensile Strength	Error	Error%
1		0%	600–610	157.254	155	2.254	1.45419355
2		0%	700	138.756	141	2.244	1.59148936
3		2%	600–610	192.754	195	2.246	1.15179487
4		2%	700	174.256	172	2.256	1.31162791

3. Experimental Work

3.1. Material Preparation

Titanium dioxide (TiO_2) and zirconia (ZrO_2) ceramic particles of 40 nm particle size were added as reinforcement materials to A356 alloy with the chemical composition illustrated in Table 2. A charge of 1 kg of aluminum alloy A356 was placed in a crucible furnace, and then heated to the required temperature (640 °C). The addition of the nanoparticles was made either at 710 °C or 640 °C in the liquid or semisolid state, respectively, by direct immersion of small packages of alumina nanoparticles wrapped in aluminum foil with simultaneous mechanical stirring of the melt. The melting and casting conditions are fully presented in previous work [16–18]. In the case of liquid state, the melt was brought to 700 °C when the addition was made, then stirred and poured. While in the case of the semisolid state, the temperature of the melt was brought down to 600 °C before pouring. The nanoparticles were added, while the melt was stirred mechanically at varied stirring speeds of (270, 800, 1500, 2150 rpm), and using the melting unit illustrated in Figure 1. The stirring was carried out mechanically using four blades impeller. The Al_2O_3 , TiO_2 and ZrO_2 nanoparticles were preheated to 700 °C, 400 °C and 500 °C, respectively, to avoid entering the sintering stage. After completion of stirring and mixing, the alloys were poured in preheated steel molds at 300 °C. Table 3 summarizes the different casting conditions used in this work.

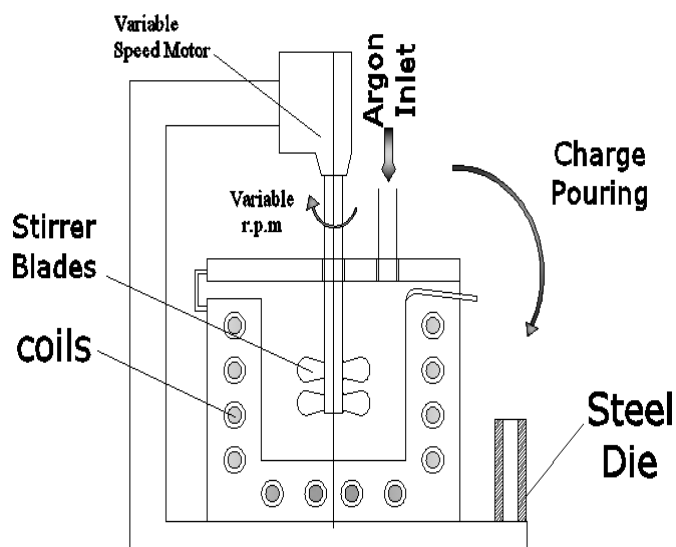


Figure 1. Furnace used for preparing the castings.

Table 2. Chemical Composition (in weight%) of A356 cast Al-Si.

Alloy	Chemical Composition (weight%)							
	Al	Si	Mg	Fe	Cu	Pb	Zn	Mn
A356	Bal.	7.44	0.3	0.27	0.02	0.022	0.01	Nil

Table 3. Casting conditions used in this work.

No.	Al ₂ O ₃ Weight%	TiO ₂ Weight%	ZrO ₂ Weight%	Temperature (°C)	Stirring Speed (rpm)
1	0	0	0	600	1500
2	1	1	1	600	1500
3	2	2	2	600	1500
4	4	3	3	600	1500
5	--	5	5	600	1500
6	2	3	3	600	270
7	2	3	3	600	800
8	2	3	--	600	2150
9	2	3	--	700	1500

--: Condition not relevant to this addition.

3.2. Mechanical Testing

The mechanical properties mainly tensile strength, ductility, and hardness were determined in the as-cast conditions for the investigated material. The tensile tests were conducted on round tension test specimens of diameter 5.02 mm and gage length 25.2 mm using a universal testing machine according to DIN 50125. The reported result for each case is the highest value among three samples. The hardness tests were conducted on Rockwell hardness testing machine using a (1/16)" diameter hardened steel ball and a 62.5 kg applied load.

3.3. Microstructure and SEM Analysis

The microstructure examination was carried out using OLYMPUS DP12 optical metallurgical microscope (New York Microscope Company, Beni Suef, Egypt) equipped with a high-resolution digital camera for investigating the microstructure. The surface topography and fracture characteristics were studied using Scanning Electron Microscope (JSM-5400 SEM, JEOL Company, Centre for Metallurgical Research CMRDI Cairo, Egypt) to understand the fracture and wear mechanisms. The favorable sites for Al₂O₃ particle incorporation were identified by Scanning Electron Microscope (JSM-7000 FEG-SEM, JEOL Company, Gemeinschaftslabor fuer elektronmikroskopie GFE, Aachen, Germany), lateral resolution 1.2 nm at 30 kV combined with EDX/EBSD-System EDAX Pegasus for chemical and crystallographic analysis. The ZrO₂ agglomerates were detected by using JSM-5410 Scanning Electron Microscope (JEOL Company, Beni Suef, Egypt) with a high-resolution of 3.5 nm.

3.4. Wear Test for the Al₂O₃ Nanoreinforced Alloy

PLINT TE 79 Multi Axis Tribometer Machine (Phoenix Tribology Limited Company, Cairo University-Giza, Giza, Egypt) was used for measuring the friction force; friction coefficient and wear rate for the manufactured materials. A standard specimen with diameter of 8 mm and 20 mm length is prepared; then a computerized pin on disc machine, used for friction and wear testing of materials, is loaded vertically downwards onto the horizontal Disc. The wear tests were then performed for the A356

cast material with the following parameters: velocity = 0.8 m/s, time = 1200 s and load = 10 N. The differences in the weight of the samples were taken as an indication of the wear resistance of the material.

4. Results and Discussion

4.1. Mechanical Properties

4.1.1. Effect of Nanoparticles Addition

Figures 2–4 present the Mechanical properties (ultimate tensile strength (UTS), elongation% and hardness) of the produced castings with Al₂O₃, TiO₂ and ZrO₂ nanoparticles reinforcement.

It can be seen from Figure 2 that as the weight% of Al₂O₃ nanoparticles increases, the UTS increases; the maximum UTS was reached (195 MPa) at 2 weight% Al₂O₃ (increase of about 26%). Beyond this limit, the UTS decreases as the weight% increases. It can also be seen that the ductility increases when Al₂O₃ exceeds 1 weight%. The ductility increases by about 40% with 2 weight% Al₂O₃ nanoparticles added. The ductility reaches a minimum value with 4 weight% Al₂O₃ nanoparticles added. It can also be noted that the hardness increases by about 30% with 4 weight% Al₂O₃ nanoparticles added.

It is shown from Figure 3 that as the weight% of the TiO₂ nanoparticles increases up to 3%, the UTS increases until reaching 185 MPa. Beyond this weight%, the UTS decreases with increase in the weight% of the TiO₂ nanoparticles. The ductility reaches its maximum with 3 weight% TiO₂ nanoparticles added, and then drops to a minimum value with 5 weight% TiO₂ nanoparticles added. The hardness reaches its minimum value of 49 HRB with the addition of 5 weight% TiO₂ nanoparticles, which means that the material becomes softer and this is supported by the drop in the strength.

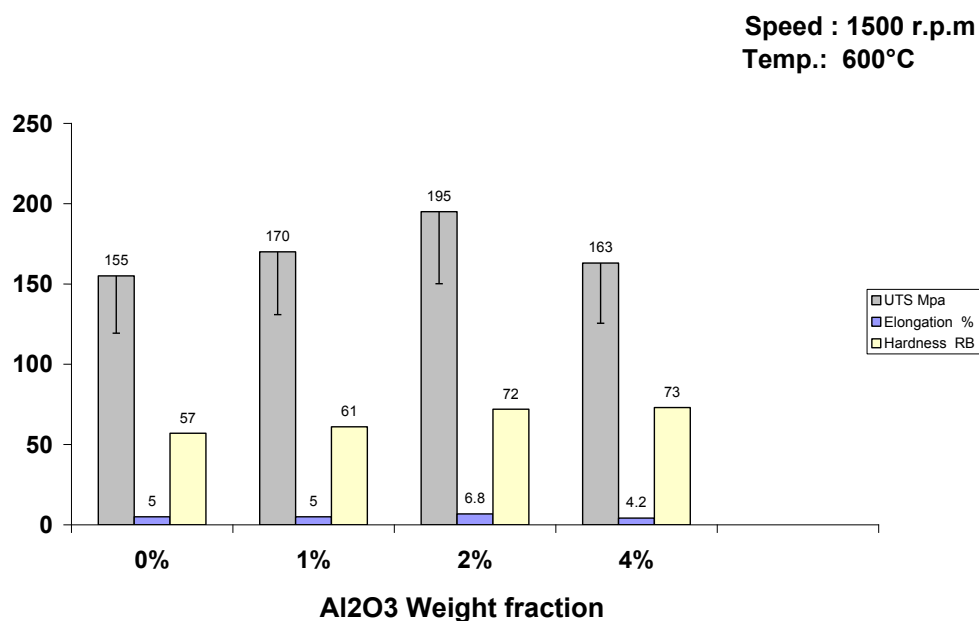


Figure 2. The effect of Al₂O₃ nanoparticles% on the ultimate tensile strength (UTS), hardness and ductility using 1500 rpm stirring speed at semi-solid state (600 °C).

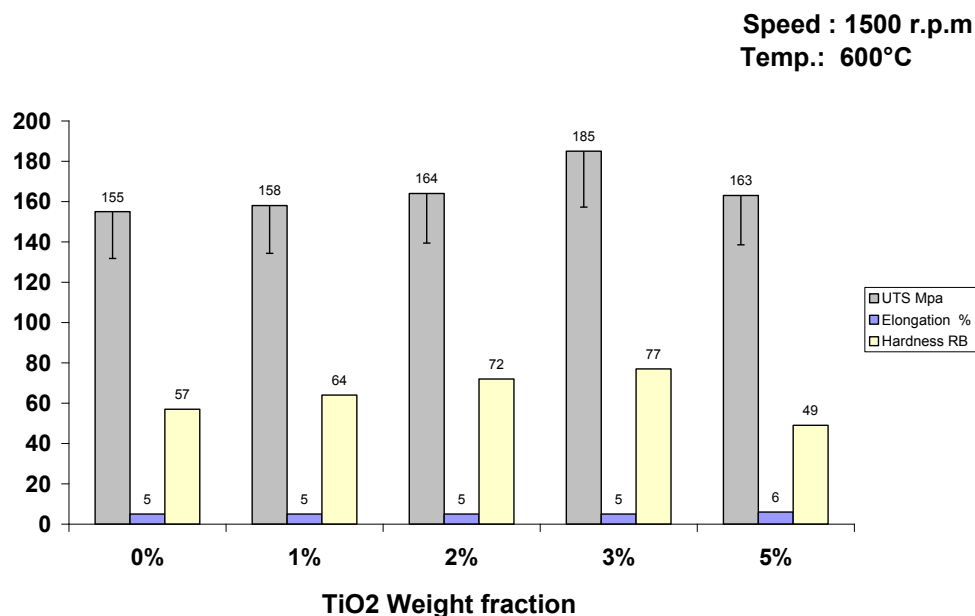


Figure 3. The effect of TiO₂ nanoparticles% on the UTS, hardness and ductility using 1500 rpm stirring speed at semi-solid state (600 °C).

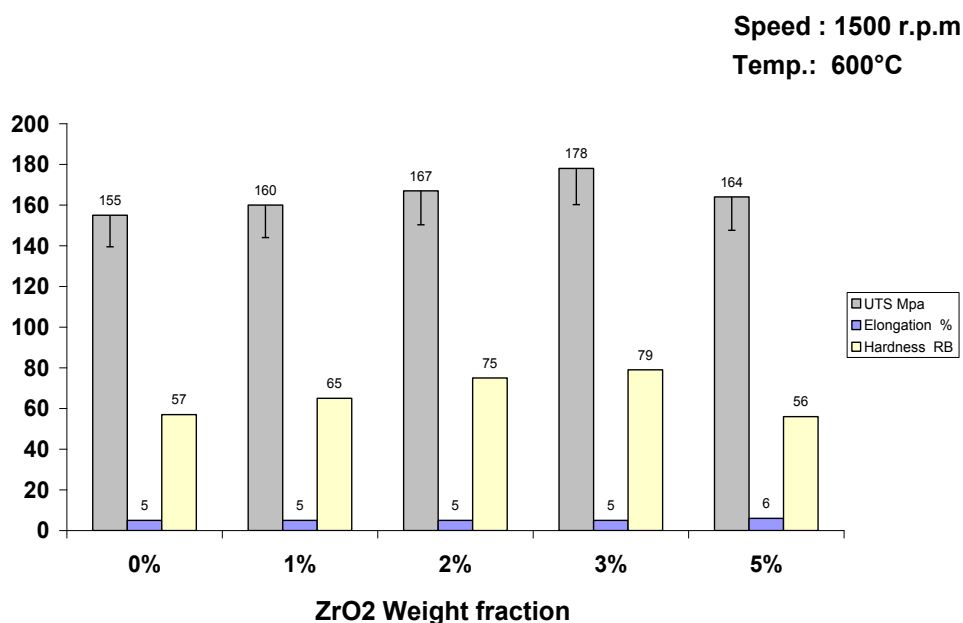


Figure 4. The effect of ZrO₂ nanoparticles% on the UTS, hardness and ductility using 1500 rpm stirring speed at semi-solid state (600 °C).

Figure 4 shows the effect of ZrO₂ nanoparticles% on the UTS using 1500 rpm stirring speed in the semi-solid state (600 °C). It can be seen that the addition of 3 weight% ZrO₂ nanoparticles results an increase in the tensile strength and the hardness. Whereas, the increase in ductility was only observed at 5 weight% ZrO₂ coupled with a decrease in both hardness and strength.

The previous results show that the inclusion of 2–3 weight% nanoparticles increases the tensile strength of the nanoreinforced A356 alloy, without loss in ductility and even an increase in ductility, in some cases. Beyond this limit all properties drop. The observed increase in the strength of the A356 nanoreinforced alloys suggests a misfit effect in the lattice parameter of the matrix phase. This would be

a result of cooling induced changes caused by the difference between the coefficients of thermal expansion between the primary phase (Al or Si) and the nanoparticles resulting an increase in the hardness of the first. The coefficients of thermal expansion are: (22.2×10^{-6} m/m K for Al, 3×10^{-6} m/m K for Si, 5.4×10^{-6} m/m K for Al₂O₃ nanoparticles, 9×10^{-6} m/m K for TiO₂ nanoparticles, and 6.53×10^{-6} m/m K for ZrO₂ nanoparticles) [27]. Additionally, enhanced dislocation generation and reduced sub grain size owing to the presence of the nanoparticles may be contributing to the increased hardness of the aluminum phase. The increase in the hardness is also due not only to the mismatch in thermal expansion, but also mismatch in elastic moduli of the nanoparticles. The addition of the nanoparticles also results in a constraint in the plastic flow of matrix. The matrix could flow only with the movement of the nanoparticles or over the particles during plastic deformation, the matrix gets constrained considerably to the plastic deformation because of smaller inter-particle distance and this results in higher degree of improvement in the flow stress.

Rapid quenching from the melt and solid state reactions have been identified as processing routes for obtaining nanostructured materials leading to two phase nanostructures, however, it is highly desirable to obtain such nanostructures directly in bulk form, e.g., through casting [28]. The current work focuses on the properties of nanodispersed A356 alloy obtained by rheocasting, which is a challenging production method for producing nanodispersed alloys. The potential for nanodispersed materials for being high-tech materials has been explored [29] and it has been shown that the addition of nano-oxides results improvement in the hardness, the tensile strength and the ductility of stir cast aluminum. This has been explained by the tendency of the oxide nanoparticles to agglomerate on the grain boundaries in columnar structures, whereas these oxide nanoparticles are more likely to disperse uniformly along the equiaxed structures resulting from stirring.

It is shown from Table 4, that alumina and zirconia have close coefficients of thermal expansion, whereas titanium oxide has a relatively higher coefficient. It is also shown that alumina and titanium oxide have higher elastic moduli, whereas zirconium oxide has the least elastic modulus among the three oxides. This may explain the difference in the obtained strength results for the three castings as the alloy reinforced with alumina shows higher strength compared to that dispersed with zirconia.

Table 4. Properties of Al₂O₃, TiO₂ and ZrO₂ Reinforcement Nanoparticles.

Reinforcement	γ -Al ₂ O ₃ *	TiO ₂ *	ZrO ₂ *
Density (g/cm ³)	3.60	4.23	5.89
Crystal Structure	FCC	Tetragonal	monoclinic
Appearance	White Solid	White solid	White powder
Young's Modulus (GPa)	380	244	171
Average Size (nm)	50	50	50
Melting point °C	2054	1870	2715
Thermal conductivity, at 800 °C, W/m °K	29	8	5.5
Coefficient of thermal expansion (10 ⁻⁶ m/m °K)	5.4	9	6.53

* CRC Materials Science and Engineering Handbook.

4.1.2. Effect of Stirring Speed

It can be seen, from Figure 5 that as the stirring speed increases up to 1500 rpm, the UTS increases to reach 195 MPa. Beyond this stirring speed, the UTS decreases as the stirring speed increases possibly due to the increase in internal porosity [18] and as well the semi-solid cast cooling rapidly below the ranges permitting sound castings to be obtained. Increasing the speed of stirring beyond 850 rpm increases the ductility. The ductility increases by about 45% at a stirring speed of 1500 rpm. At 2150 rpm stirring speed, the ductility reaches its minimum values; possibly due to the presence of high porosity content [18]. This could also explain that the hardness at this stirring speed decreases after reaching a maximum value at 1500 rpm.

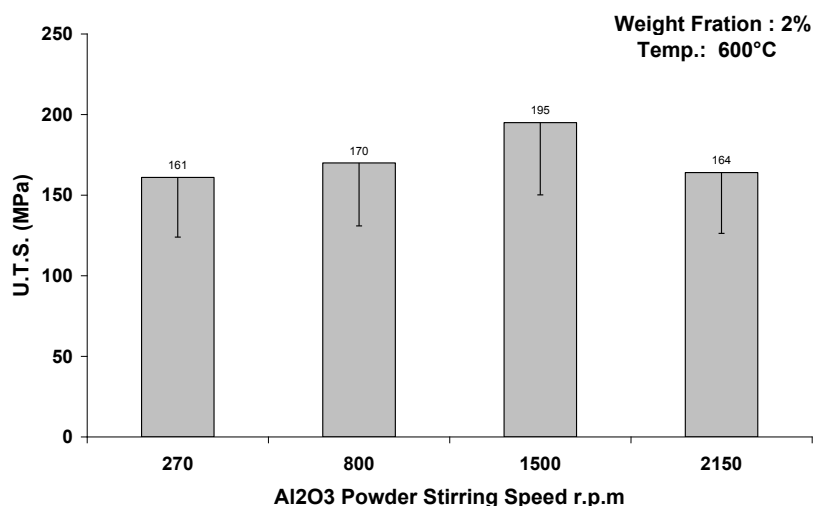


Figure 5. The effect of stirring speed on the UTS of 2 weight% Al₂O₃ nanoreinforced alloy at 600 °C.

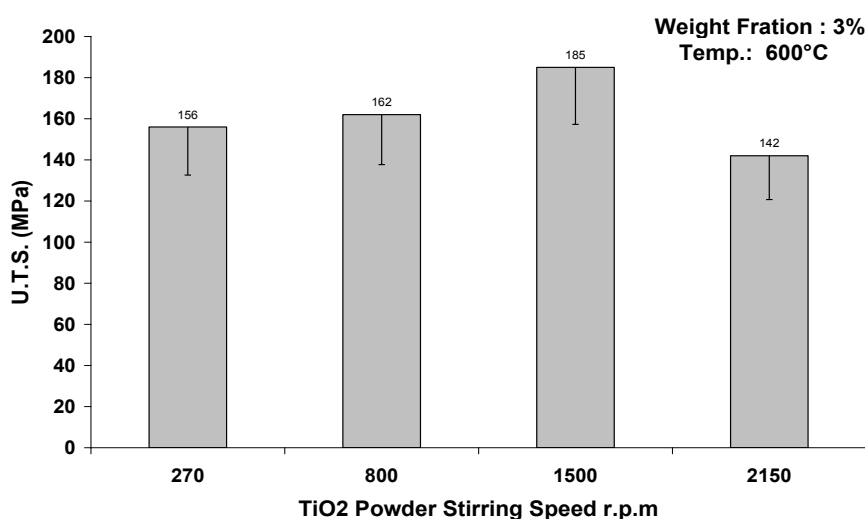


Figure 6. The effect of stirring speed on the UTS of 3 weight% TiO₂ nanoreinforced alloy at 600 °C.

It is shown in Figure 6 that as the stirring speed of nano TiO₂ reinforced casting increases to 1500 rpm, the UTS increases to reach 185 MPa. Beyond this stirring speed, the UTS decreases as the stirring speed increases, possibly due to increase in internal porosity [18] and cooling of the semi-solid slurry, as explained before. When the speed of stirring increases beyond 850 rpm, the ductility starts to

increase. The ductility increases slightly at the stirring speed of 1500 rpm. At 2150 rpm stirring speed, the ductility reaches its minimum value; possibly due to the high porosity [18] content created in the composite. Again, the hardness at this stirring speed decreases after reaching its maximum value at 1500 rpm.

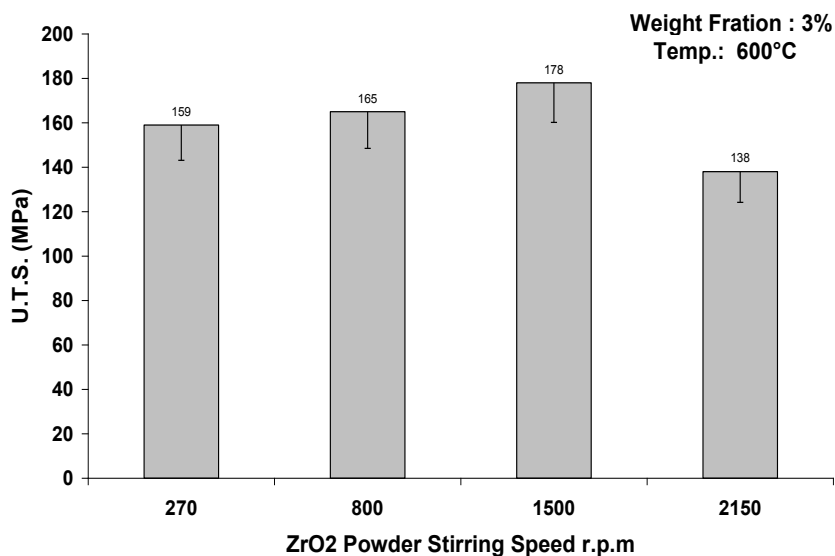


Figure 7. The effect of stirring speed on the UTS of 3 weight% ZrO₂ nanoreinforced alloy at 600 °C.

Figure 7 shows that as the stirring speed of the ZrO₂ nanoreinforced material increases to 1500 rpm, the UTS increases to reach 192 MPa. Beyond this stirring speed, the UTS decreases as the stirring speed increases, possibly due to internal porosity [18] and faster cooling of the slurry. At 2150 rpm stirring speed, the ductility reaches its minimum values, possibly due to the high porosity content [18] created in the casting, where its hardness at this stirring speed decreases after reaching its maximum value at 1500 rpm.

4.1.3. Effect of Casting Temperature

Figure 8 shows that the max. UTS is achieved for all conditions for the casting poured from 600 °C with stirring. This could be explained by the beneficial effect of the semi-solid state (mushy zone) on the distribution of the nanoparticles through the A356 matrix, which leads to enhanced reinforcement of the matrix. The good distribution of the particles leads to higher UTS and higher ductility with noticeable change in the hardness values. The improved strength and ductility exhibited by the nanoreinforced alloy cast from the semi-solid state compared to that cast from the liquid state (700 °C) is attributed to the high effective viscosity of the metal slurry that prevents particles from settling, floating, or agglomerating.

The known models addressing the incorporation of particles into a solidifying matrix have been identified [30] to be: (i) the kinetic models based on the interaction between the velocity of the solid/liquid interface and the velocity of the particle; (ii) the thermodynamic models which are closely related to classical heterogeneous nucleation theory; and (iii) the models based on the ratio of the thermophysical properties of the particles and the melt. A good correlation among all three models [31] has integrated many of the effective parameters, and has suggested that there are three possible pathways for nanoparticle capture: viscous capture, Brownian capture and spontaneous capture. Viscous capture

occurs under conditions of extremely high cooling rates or increased viscosity of the melt. Brownian capture is likely to occur when the nanoparticles have slightly lower Hamaker constants than the melt. Spontaneous capture was proposed as the most favorable for nanoparticle capture during solidification of metal melt, the key being to select or design/fabricate suitable nanoparticles that offer a higher Hamaker constant than that of the liquid metal [30]. However, the problem with these models is that they consider capturing of the nanoparticles, but ignore strengthening mechanisms for the proposed matrix/reinforcement combinations.

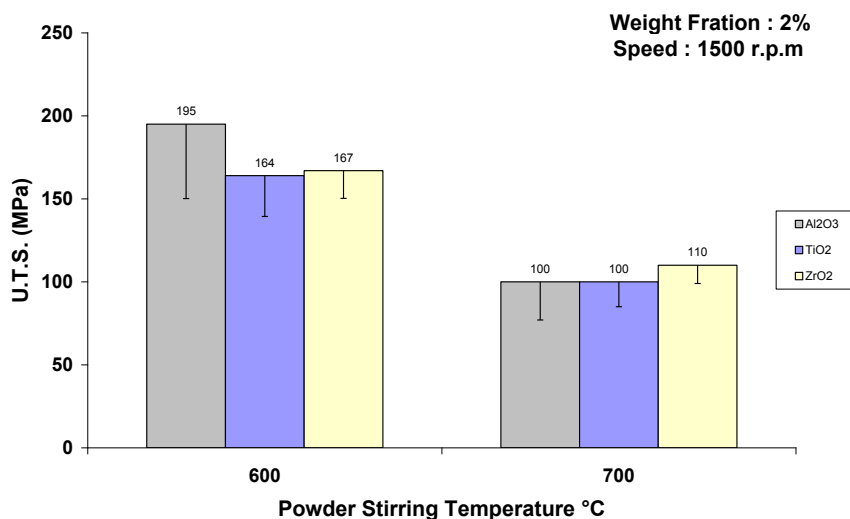


Figure 8. The effect of stirring temperature on the UTS at 1500 rpm stirring speed.

This work as well as others have shown that adding nanoparticles to metal matrix of A356 (and A390 [19]) has significant potential of enhancing both strength and ductility. It has been shown [24] that in eutectic and hypereutectic matrix alloys, such as Al-Si, particle capture take place for all growth conditions, whereas, in hypoeutectic Al alloy systems, where a non-planar solid-liquid interface is typically present, particle pushing takes place. The classical theory for strengthening in dispersed structures forming composites [24] is based on the dislocation motion being constrained by the precipitates and dispersoid particles. These particles form coherency strains and dislocation networks around them, leading to a misfit between the particles and the matrix, which causes the hardness and strength to increase. The usual drop in ductility associated with increase in strength is explained by the fact that dislocations move on specific slip planes under the action of a shear stress. If the slip plane has obstacles penetrating it, e.g., precipitates or dispersoids, a dislocation moving on this slip plane must interact with these obstacles. The high volume fraction of interfacial regions offered by the nanodispersion cause the improvement in ductility where grain boundary sliding becomes the major deformation mechanism [28].

4.2. Microstructural Evolution

Figure 9a–c shows the optical microstructure of the base matrix A356 and the alloys reinforced with 2 weight% Al₂O₃ and 3 weight% TiO₂, using stir casting (rheocast), respectively. The typical microstructure for this alloy consists of primary aluminum matrix (white phase) and Al-Si eutectic (dark lamellar structure). The as-cast microstructures of the three castings show that the phases are uniformly

distributed. The figures clearly show a morphological change in the microstructure. In the base matrix sample, the microstructure is dendritic, whereas in the other rheocast samples, the primary dendrites are fragmented due to mechanical stirring. However, with the continued stirring, the plastic strains within the fragmented grains would be considerably less and the process of coarsening will start (ripening effect) [13]. Since the coarsening is driven by interfacial energy, the process will lead to a reduction in the surface area and eventually spheroidal morphology is obtained. It was observed that not only the primary Al grains (white portions) but also eutectic Si particles (dark portions) are globular in rheocast samples in comparison to the base matrix, without stirring, cast samples. As the structure contains good amount of eutectic phases it should give a range of mechanical properties with mechanical stirring during processing [13]. The microstructure observations well support the results of the mechanical properties of the alloys reinforced with nanoparticles using mechanical stirring. The observed refinement of the Si eutectic has been also observed and recorded before [22] and has been attributed to the improved nucleation of Si particles and depletion of Si element near the Si particles [22]. However, the authors [22] have attributed this effect to heterogeneous nucleation initiated by the γ -Al₂O₃ nanoparticles. The effect on modifying the eutectic Si has been attributed to the result from the effect of the pushed γ -Al₂O₃, during solidification into the remaining melt, on restricting growth of the particles.

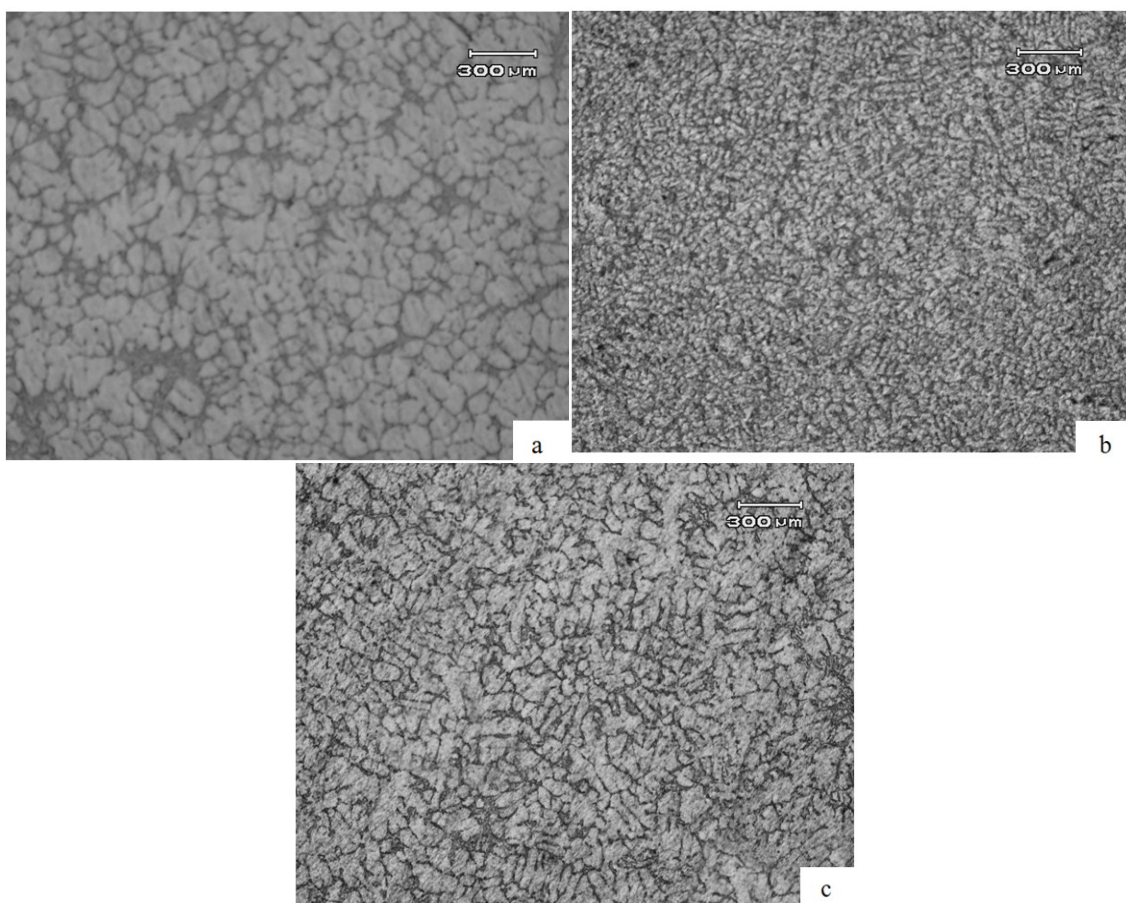


Figure 9. (a) Microstructure of the A356 matrix alloy with no stirring. (b) Microstructure of A356 nanoreinforced with Al₂O₃. (c) Microstructure of A356 nanoreinforced with TiO₂.

Stirring as an external applied force is believed to bring thermal homogeneity within the semi-solid slurry establishing shallow temperature gradients that alleviate nucleation barrier within the bulk liquid. In addition, stirring may assist in disintegration of the secondary and tertiary dendrite arms. Such phenomenon is the main recipe for equiaxed grain growth in SSM cast billets with distinct deformation and flow characteristics [14].

Figure 10 represents the microstructure of the A356 matrix alloy reinforced with 2 weight% Al_2O_3 at 600 °C with different stirring speeds. Figure 10a illustrates the presence of large grains of primary α -Al caused by low stirring at 270 rpm, which causes poor mechanical properties. When the stirring speed increases, this results in finer grains, which lead to an improvement in the mechanical properties of the castings represented by microstructures in Figure 10b,c.

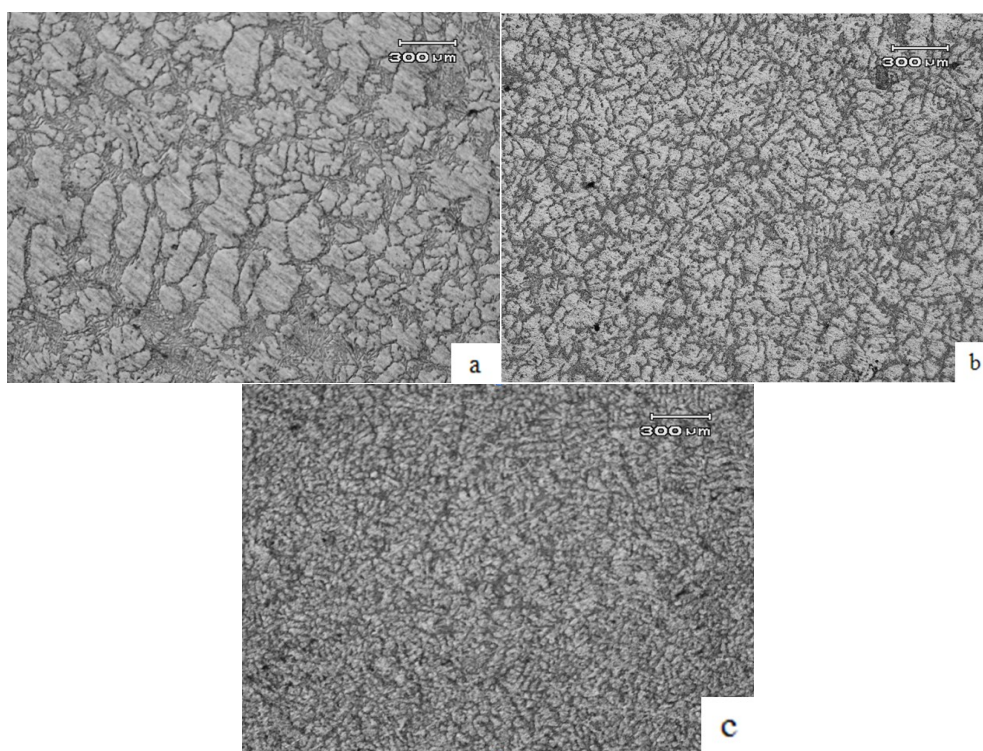


Figure 10. The microstructure obtained for different stirring speeds for the casting reinforced with 2 weight% Al_2O_3 at 600 °C: (a) 270 rpm; (b) 800 rpm; and (c) 1500 rpm.

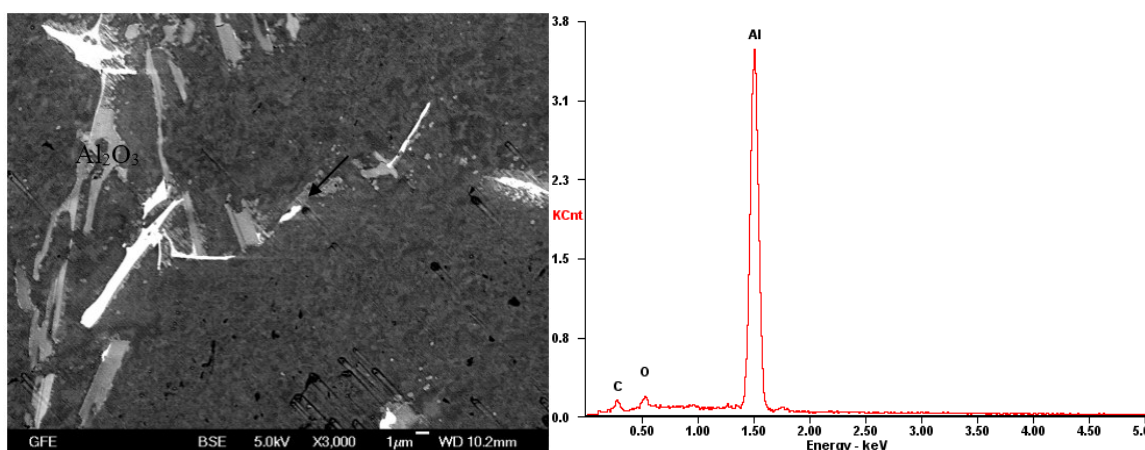


Figure 11. The SEM (left) and EDX (right) for the Al- Al_2O_3 nano-reinforced matrix.

Figure 11 shows the SEM and EDX for the Al-Al₂O₃ nano-reinforced matrix, which clearly shows the existence of the Al₂O₃ dispersed nano-particles in the Al-Matrix.

Figure 12 illustrates the microstructure of the A356 matrix alloy reinforced with 3 weight% ZrO₂ at 600 °C with 270 rpm stirring speed. Figure 12 shows the presence of large grains of primary α -Al resulting from the low stirring speed which causes poor mechanical properties.

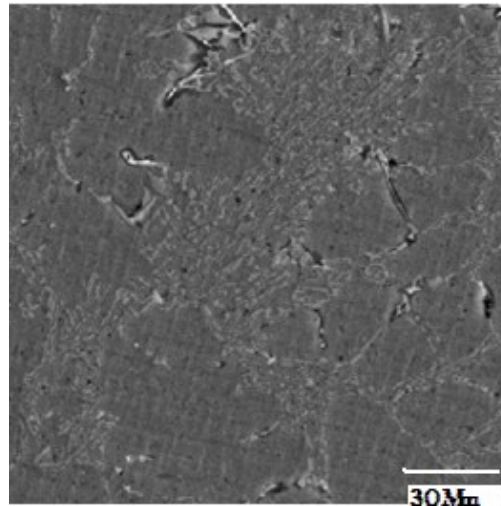


Figure 12. The microstructure of A356 reinforced with 3 weight% ZrO₂ at 270 rpm stirring speed.

Figure 13 shows the SEM fracture surface of the A356 alloy containing Al₂O₃, on which the agglomerated particles are detected. Agglomeration of nano-particles occurs during the melting stage and results in non-homogenous distribution inside the matrix. The Al₂O₃ agglomerated particles have a size of about 3 μ m and are located in the interdendritic spaces, attached to the matrix. The EDXS analysis confirmed that these are Al₂O₃ particles, though a strong reflection from the matrix was inevitable.

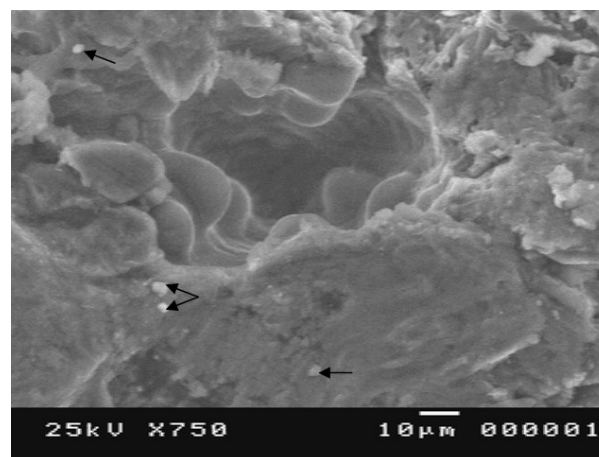


Figure 13. SEM for A356 Alloy containing Al₂O₃ agglomerated particles.

Figure 14 illustrates the brittle fracture surface of the specimen of the A356 alloy reinforced with 3 weight% TiO₂, which showed the optimum mechanical properties. It was difficult to detect TiO₂ nanoparticles; possibly due to the absence of agglomerated particles, which could appear clearly with the Al₂O₃ agglomerated particles.

Figure 15 shows the SEM of the A356 alloy containing ZrO_2 nanoparticles that have agglomerated during the melting stage, leading to a drop in the mechanical properties.

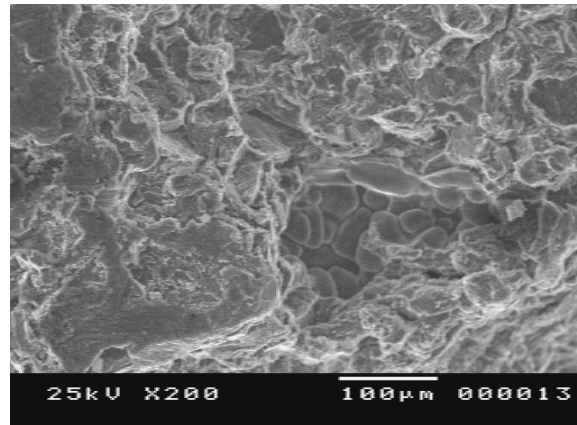


Figure 14. The (SEM) of the fracture surface specimen reinforced with 3 weight% TiO_2 nanoparticles.

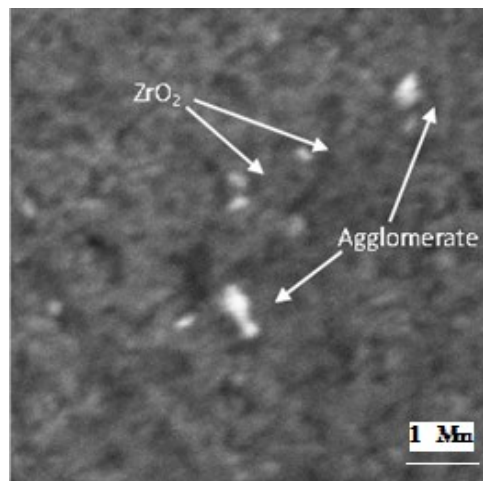


Figure 15. SEM for A356 Alloy containing ZrO_2 agglomerated particles.

4.3. Wear Test Results

The average-wear results of A356 samples reinforced with 0, 1, 2 and 4 weight% Al_2O_3 nanoparticles are shown in Table 5. It can be seen from Table 5 that the addition of 1 weight% nanoparticles resulted in a significant drop in friction coefficient, unaccompanied by any improvement in terms of weight loss. Increasing nanoparticles up to 4% resulted deterioration in wear resistance in terms of friction coefficient and weight loss.

Table 5. The average wear results of A356 samples reinforced with 0, 1, 2 and 4 weight% Al_2O_3 nanopowder.

Sample No.	Additions	Weight Loss (mg)	Friction Coefficient
1	A356	3.9	0.4
2	A356 + 1% Al_2O_3	4.0	0.361
3	A356 + 2% Al_2O_3	4.5	0.385
4	A356 + 4% Al_2O_3	5.5	0.430

The results show that the addition of 1 weight% nanoparticles did not produce a significant change in the wear resistance of the hypo-eutectic alloy A356, though there was a reduction in the friction coefficient. The fact that the wear resistance deteriorated after adding 2 and 4 weight% nanoparticles (though the hardness and strength increased) may be attributed to microstructural effects as well as the high load used in the test. Previous work on A390 alloy [19] has shown that the wear resistance of nanoreinforced A390 was enhanced compared to monolithic A390 alloy, which has been attributed to higher hardness resulting from refinement in microstructural constituents. This behavior is also attributed to microstructural effects in both alloys, where nano additions promote Al phase formation for the hypoeutectic alloys, whereas their refining effect is more pronounced for the hypereutectic alloys. The main wear mechanism observed [19] was delamination and tearing. Other work [32] has reported enhancement in the wear resistance of A356 rheocast alloy compared to those obtained by conventional casting, which has been attributed to the equiaxed structure obtained by rheocasting. The main wear mechanism was found to be plowing at small stresses and mixed plowing and delamination at high stresses. However, no data has been found to evaluate the wear performance of the rheocast nanodispersed A356 alloy.

The samples subjected to wear tests have been examined using SEM. Figure 16 show clearly the Al_2O_3 nanoparticles agglomerates distributed on the surface of the samples with 1 and 2 weight% Al_2O_3 addition subjected to wear, respectively. The figures also show that the dominant wear mechanism was a combination of adhesion and delamination mechanisms, similar to findings in a previous work for hypereutectic Al-Si alloy A390 [19].

In the base matrix sample without stirring, the microstructure is dendritic, whereas in the other rheocast samples, the primary dendrites are fragmented due to mechanical stirring which explains the improvement in the mechanical properties. Analysis using both scanning electron microscope (SEM) and high magnification shows evidence for the possibility of incorporating and entrapping nanosized particles within the interdendritic interface developing during the solidification of the dispersed alloys.

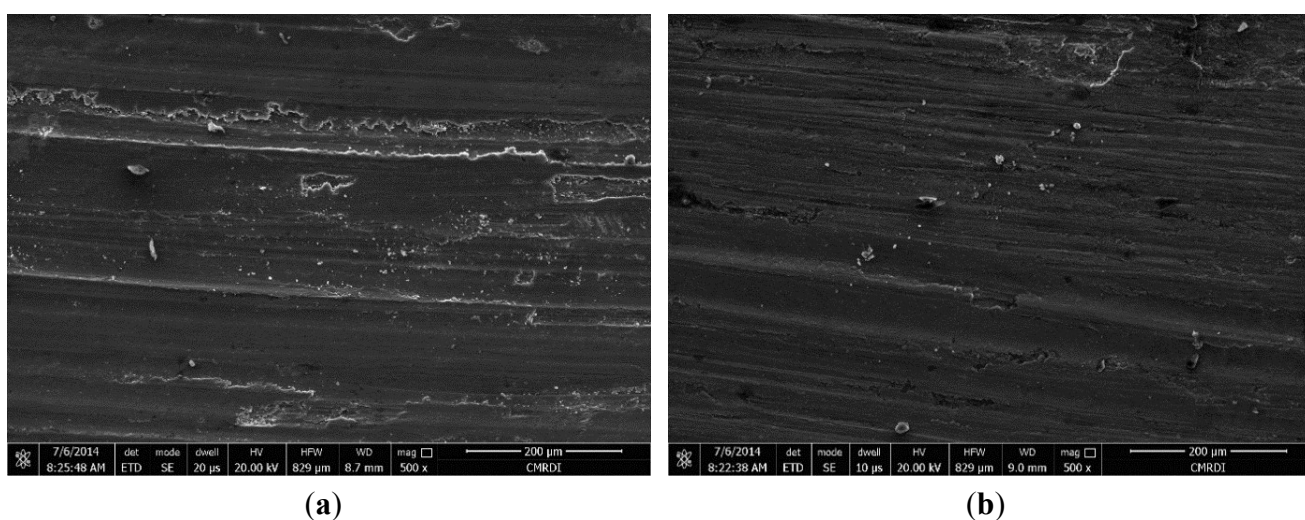


Figure 16. SEM for wear surface of (a) 1 weight% Al_2O_3 and (b) 2 weight% Al_2O_3 nanoparticles.

The difference between the wear performance of the nanodispersed hyper- [19] and hypo-eutectic alloys (reported in this work) may be explained by the effect of the nanoparticles additions on both

alloys. The addition of nanoparticles promotes the formation of α -Al phase and has been attributed to the improved nucleation of Si particles and depletion of Si element near the Si particles [19,33]. This would produce a deterioration effect on the wear resistance of the hypo-eutectic alloys, whereas the effect would be less significant on the hyper-eutectic alloys, since the morphology of the Si particles and the shape of the α -Al, as well as the morphology of the eutectic Si have a major contribution. It has been stated [19,33] that the cracks easily initiate inside the brittle primary Si or eutectic Si, and then propagate through boundaries with α -Al phase, thus the change in the Si morphology (according to restricted nucleation and growth theory of modification), and the crystalline appearance of the α -Al phase would improve the wear resistance for the hyper-eutectic alloys [33]. Also, the addition of nanoparticles to the hypereutectic alloys has been shown to produce a refining effect on the primary silicon particles, which has been attributed to increasing the nucleation sites [19] or inducing a thermal sub-cooling effect.

It has been shown [18,19] that nanodispersed aluminum alloys have refined microstructural constituents (Al dendrites, interlamellar spacing and primary Si particles) compared to their monolithic counterparts. The mechanical strength of crystalline metals or alloys is largely controlled by the grain size d . The well-known empirical Hall–Petch equation relates the yield strength σ_y to the average grain size d according to $\sigma_y = \sigma_0 + k(d)^{-1/2}$. Where σ_0 is the friction stress and k is a constant. A similar relation exists between the hardness and the grain size. Consequently, reducing d to the nanometer regime increases the strength considerably. However, the limits of the conventional description of yielding and of new mechanisms that may come into play at these small dimensions need to be explored and studied in much more detail [28].

Although the mechanisms operative in the nanoscale grain size regime differ from those for coarse-grained materials, strengthening mechanisms that are well documented for coarse-grained metals and alloys can also operate in nanocrystalline metals and alloys, although modified by the nano-scale grain size and non-equilibrium microstructures [34]. It is suggested that the smaller sizes of nanoparticles are expected to contribute to Orowan hardening; while the very large sizes (or agglomerates) would likely produce rule-of-mixtures behavior. Nanodispersed cast structures carry both natures of composites and refined structures. It is important at this stage to understand the active strengthening mechanisms in these materials, as this will be the key to developing new structures.

A new model has been recently suggested considering that the high mechanical resistance of nanoreinforced composites is the result of the incremental summation of several strengthening mechanism contributions, namely: load transfer effect, Hall-Petch strengthening, Orowan strengthening, coefficient of thermal expansion (CTE) and elastic modulus (EM) mismatch [35]. The new proposed model was shown to be consistent with experimental data for the system Al/2weight% Al₂O₃ [35].

5. Conclusions

- The castings made by adding nano-sized dispersoids using semi-solid route exhibited higher strength and ductility when compared with those prepared by liquid metallurgy route.
- The stirring speed has a significant effect on the mechanical properties of the nano-dispersed castings. Increasing stirring speed more than 1500 rpm causes reduction in the tensile strength. The alloy stirred with 1500 rpm exhibits the highest tensile strength and elongation%.

- The A356 matrix alloy reinforced with 2% weight of Al₂O₃ showed the highest strength properties when compared with the one reinforced with 3% ZrO₂ weight and 3% weight of TiO₂ nano particles at the conditions of 1500 rpm stirring speed at semi solid state temperature 600 °C. In all cases this was not combined with loss in ductility.
- Analysis using scanning electron microscope (SEM) at high magnification shows evidence for the possibility of incorporating and entrapping nano-sized particles within the interdendritic interface developing during the solidification of the dispersed alloys.
- The introduction of varying amounts of nanosized particles to the A356 alloy did not produce a significant change on the wear resistance of the tested hypo-eutectic alloy A356 material with 1% nanoparticles and resulted deterioration after adding 2% and 4% nanoparticles, though a drop in the friction coefficient occurred at 1% addition.
- The options for making nanodispersed cast alloys still meet the challenge of obtaining homogeneous distribution of the nanoparticles.
- Another challenge is quantifying the amount of nanoparticles entering the slurry.

Acknowledgments

The authors would like to acknowledge the role of late -Ing. Y. Shash, the head of Mechanical Design and Production Dept., Faculty of Engineering, Cairo University who advised and supported this work at its early stages.

Author Contributions

Iman El-Mahallawi has led the research group, designed and performed the experiments for casting preparation, and microstructural and mechanical properties investigation for the Al oxide nanoreinforced material and wrote the introduction and discussion parts of the paper. Ahmed Shash has designed and performed the experiments of casting preparation, and microstructural and mechanical properties investigation for the Ti oxide nanoreinforced material and wrote the relevant parts. Amer Eid Amer has designed and performed the experiments of casting preparation, and the microstructural investigations for the Zr oxide nanoreinforced material and wrote the relevant parts.

Conflicts of Interest

The authors declare no conflict of interest.

References

1. Kashyap, K.T.; Muralli, S.; Raman, K.S.; Murthy, K.S.S. Casting and heat treatment variables of Al-7Si-Mg alloy. *Mater. Sci. Technol.* **1993**, *9*, 189–203.
2. Gruzleski, J.E.; Closset, B.M. *The Treatment of Liquid Aluminuim-Silicon Alloys*; AFS: Des Plaines, IL, USA, 1990; pp. 107–126.
3. Cacers, C.H. Microstructure effects on the strength-ductility relationship of Al-7Si-Mg casting alloys. *Mater. Sci. Forum* **2000**, *331*, 223–228.

4. Rooy, E.L. Aluminum and aluminum alloys. In *ASM Metals Handbook*; Aluminum Company of America: New York, NY, USA, 1992; Volume 15.
5. Shi, W.; Gao, B.; Tu, G.; Li, S.; Hao, Y.; Yu, F. Effect of neodymium on primary silicon and mechanical properties of hypereutectic Al-15%Si alloy. *J. Rare Earths* **2010**, *28*, 367–370.
6. Chen, C.; Liu, Z.; Ren, B.; Wang, M.; Weng, Y.; Liu, Z. Influences of complex modification of P and RE on microstructure and mechanical properties of hypereutectic Al-20Si alloy. *Trans. Nonferrous Met. Soc. China* **2007**, *17*, 301–306.
7. Dahle, A.K.; Nogita, K.; McDonald, S.D.; Dinnis, C.; Lu, L. Eutectic modification and microstructure development in Al–Si Alloys. *Mater. Sci. Eng. A* **2005**, *413–414*, 243–248.
8. Cruz, K.S.; Meza, E.S.; Fernandes, F.A.P.; Quaresma, J.M.V.; Casteletti, L.C.; Garcia, A. Dendritic arm spacing affecting mechanical properties and wear behavior of Al–Sn and Al–Si alloys directionally solidified under unsteady-state conditions. *Metall. Mater. Trans. A* **2010**, *41*, 972–984.
9. Mehrabian, R.; Riek, R.G.; Flemings, M.C. Preparation and casting of Metal-Particulate Non-Metal Composites. *Metall. Trans.* **1974**, *5*, 1899–1905.
10. Eliasson, J.; Sandstorm, R. *Applications of Aluminium Matrix Composites, Part I*; Newaz, G.M., Neber-Aeschbacherand, H., Wohlbier, F.H., Eds.; Trans. Tech. Publications: Pfaffikon, Switzerland, 1995; pp. 3–36.
11. Rohatgi, P.K.; Asthana, R.; Das, S. Solidification, Structure and Properties of Cast Metal-Ceramic Particle Composites. *Int. Met. Rev.* **1986**, *31*, 115–139.
12. Singh, J.; Alpas, A.T. Elevated temperature wear of Al6061 and Al6061 20% Al₂O₃. *Scr. Metall. Mater.* **1995**, *32*, 1099–1105.
13. Seyed Reihani, S.M. Processing of squeeze cast Al6061–30vol% SiC composites and their characterization. *Mater. Des.* **2006**, *27*, 216–222.
14. Amirkhanlou, S.; Niroumand, B. Development of Al356/SiCp cast composites by injection of SiCp containing composite powders. *Mater. Des.* **2011**, *32*, 1895–1902.
15. Jerome, S.; Ravisankar, B.; Kumar Mahato, P.; Natarajan, S. Synthesis and evaluation of mechanical and high temperature tribological properties of in-situ Al–TiC composites. *Tribol. Int.* **2010**, *43*, 2029–2036.
16. El Mahallawi, I.S.; Egenfeld, K.; Kouta, F.H.; Hussein, A.; Mahmoud, T.S.; Rashad, R.M.; Shash, A.Y.; Abou-AL-Hassan, W. Synthesis and Characterization of New Cast A356/(Al₂O₃) p Metal Matrix Nano- Composites. In Proceedings of the 2nd Multifunctional Nanocomposites & Nanomaterials: International Conference& Exhibition MN2008, Cairo, Egypt, 11–13 January 2008.
17. El-Mahallawi, I.; Shash, Y.; Egenfeld, K.; Mahmoud, T.; Rashad, R.; Shash, A.; El Saeed, M. Influence of Nano-dispersions on Strength Ductility Properties of Semi-solid Cast A356 Al Alloy. *Mater. Sci. Technol.* **2010**, *26*, 1226–1231.
18. El-Mahallawi, I.; Abdelkader, H.; Yousef, L.; Amer, A.; Mayer, J.; Schwedt, A. Influence of Al₂O₃ nanodispersions on microstructure features and mechanical properties of cast and T6 heat-treated Al Si hypoeutectic alloys. *Mater. Sci. Eng. A* **2012**, *556*, 76–87.
19. El Mahallawi, I.; Shash, Y.; Rashad, R.M.; Abdelaziz, M.H.; Mayer, J.; Schwedt, A. Hardness and Wear Behavior of Semi-Solid Cast A390 Alloy Reinforced with Al₂O₃ and TiO₂ Nanoparticles. *Arab. J. Sci. Eng.* **2014**, *39*, 5171–5184.

20. Mazahery, A.; Baharvandi, H.R.; Abdizadeh, H. Development of high performance A356-nano Al₂O₃ composites. *Mater. Sci. Eng. A* **2009**, *518*, 23–27.
21. Sajjadi, S.A.; Ezatpour, H.R.; Beygi, H. Comparison of microstructure and mechanical properties of A356 aluminum alloy/Al₂O₃ composites fabricated by stir and compo-casting processes. *Mater. Sci. Eng. A* **2011**, *528*, 8765–8771.
22. Choi, H.; Konishi, H.; Li, X. Al₂O₃ nanoparticles induced simultaneous refinement and modification of primary and eutectic Si particles in hypereutectic Al–20Si alloy. *Mater. Sci. Eng. A* **2012**, *541*, 159–165.
23. Haizhi, Y. An overview of the development of Al-Si-alloy based material for engine applications. *J. Mater. Eng. Perform. JMEPEG* **2003**, *12*, 288–297.
24. Chawla, K.K. *Metal Matrix Composites*; Springer: Berlin, Germany, 2006.
25. Prabu, S.B. Influence of stirring speed and stirring time on distribution of particles in cast MMC. *J. Mater. Process. Technol.* **2006**, *171*, 268–273.
26. Shash, A.Y.; Sc, M. Effect of Processing Parameters on the Mechanical Characteristics of A356/(Al₂O₃)_p Cast Metal Matrix Nano-Composites (MMNCs). Master's Thesis, Cairo University, Cairo, Egypt, 2007.
27. Shackelford, James F.; Alexander, W. "Frontmatter" *Materials Science and Engineering Handbook*; Shackelford, J.F., Alexander, W., Eds.; CRC Press LLC: Boca Raton, FL, USA, 2001.
28. Koch, C.C. *Nanostructured Materials, Processing Properties, and Potential Applications*; CRC Press: Boca Raton, FL, USA, 2002; pp. 423–526.
29. Kim, G.; Hong, S.; Lee, M.; Kim, S.; Ioka, I.; Kim, B.; Kim, I. Effect of oxide dispersion on dendritic grain growth characteristics of cast aluminum alloy. *Mater. Trans.* **2010**, *51*, 1951–1957.
30. Boostani, A.F.; Tahamtan, S.; Jiang, Z.Y.; Wei, D.; Yazdani, S.; Khosroshahi, R.A.; Mousavian, R.T.; Xu, J.; Zhang, X.; Gong, D. Enhanced tensile properties of aluminium matrix composites reinforced with graphene encapsulated SiC nanoparticles. *Compos. Part A* **2015**, *68*, 155–163.
31. Xu, J.Q.; Chen, L.Y.; Choi, H.; Li, X.C. Theoretical study and pathways for nanoparticle capture during solidification of metal melt. *J. Phys. Condens. Matter* **2012**, *24*, 255304.
32. Dey, A.K.; Poddar, P.; Singh, K.K.; Sahoo, K.L. Mechanical and Wear Properties of Rheocast and Conventional Gravity Die Cast A356 Alloy. *Mater. Sci. Eng. A* **2006**, *435–436*, 521–529.
33. El Mahallawi, I.; Othman, O.A.; Abdelaziz, M.H.; Raed, H.; El-Fatah, T.A.; Ali, S. Understanding the role of nanodispersions on the properties of A390 Hyper-Eutectic Al-Si cast alloy. *TMS Light Met.* **2014**, doi:10.1002/9781118888438.ch227.
34. Scattergood, R.O.; Koch, C.C.; Murty, K.L.; Brenner, D. Strengthening mechanisms in nanocrystalline alloys. *Mater. Sci. Eng. A* **2008**, *493*, 3–11.
35. Casati, R.; Vedani, M. Metal Matrix Composites Reinforced by Nano-Particles—A Review. *Metals* **2014**, *4*, 65–83.